THE JOURNAL OF PHYSICAL CHEMISTRY C

ARTICLE

pubs.acs.org/JPCC

Surface and Electronic Properties of Hydrogen Terminated Si [001] Nanowires

Yuki Matsuda,[†] Jamil Tahir-Kheli,[†] and William A. Goddard , III[†,‡,*]

[†]Materials and Process Simulation Center, California Institute of Technology, California 91125, United States

[‡]Graduate School of EEWS (WCU), Korea Advanced Inst. Science Technology, Daejeon, Korea

Supporting Information

ABSTRACT: The calculated band gaps reported previously for silicon nanowires (SiNW) have disagreed with the experimental values both in magnitude and in the behavior with radius. We resolve this discrepancy here. We report ab initio quantum mechanical calculations of hydrogen terminated Si [001] nanowires (H−SiNWs) as a function of diameter (d) and hydrogen coverage using the B3LYP density functional. For smaller diameters ($d \leq 1.9$ nm) we find that the most stable surface is fully saturated with hydrogen leading to direct band gaps. For larger diameters, the surface dangling bonds are not saturated, leading to surface LUMO and HOMO states that lower the gap and lead to an indirect band gap. This transition from direct to indirect gap resolves the previous disagreement in the scaling of band gap with diameter. We conclude that the electronic properties of Si NW depend sensitively on controlling the diameter and surface hydrogen coverage.

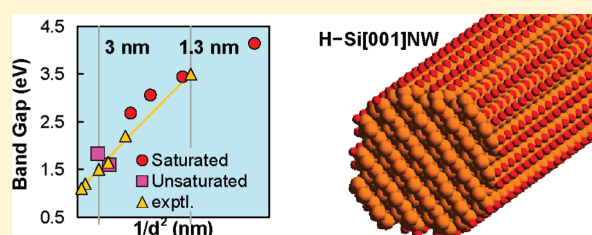

INTRODUCTION

Fabrication techniques for silicon nanowires (SiNWs) now provide precise control of the NW diameter and the crystallographic direction of the NW axis.[1−18] It is likely that the next-generation electronic devices will exploit these advances to tune SiNW electronic properties for post CMOS materials. Indeed, p-type SiNWs with diameters ≤20 nm have been recently shown to have a thermoelectric figure of merit of ZT ≈ 1, whereas the bulk value is ZT = 0.014.[1,2]

Top-down synthesis of large arrays of SiNWs of arbitrary diameter and orientation has been demonstrated using the superlattice nanowire pattern transfer (SNAP) method,[3] a very general approach for patterning silicon wafers or films to form logic circuits (multiplexer)[4] and chemical sensors.[5]

Bottom-up approaches to growing SiNWs have been demonstrated on metal catalysts (e.g., Au clusters) for diameters as small as 1.3 nm.[6] Applications of such NWs in electronics,[7] biological[8] and chemical[9] sensors, photonics,[10] and solar cells[11] using doped, coated, or functionalized NWs[12] have been reported. The Langmuir−Blodgett approach[13] and layer-by-layer assembly processes[14] have also been successful, whereas catalyzed growth seems to exhibit orientation dependence.[15−18]

However, there remain fundamental questions of how the properties of SiNWs depend upon size, number, and location of defects, and surface modifications. In addition, uncertainties about the relationship between the structural stability and surface properties become important at nanoscale dimensions due to the large surface to bulk ratio in SiNWs.

For example, normal processing of Si wafers leads to a thermal oxide that tends to provide a passive, stable, and reproducible system. However, for small NWs, the thickness of the oxide film may become comparable to the diameter leading to undesirable surface electronic effects. Thus alternative ways to passivate the silicon surface may be necessary. One such method is chemical etching of silicon in an HF treatment that terminates the surface with H.[6,19] Alternatively, etching with low energy electrons in a gas of H_2, leads to H termination of the surfaces.

In this work, we report the electronic properties of SiNWs oriented along the [001] direction as a function of diameter and surface composition. These properties are derived from quantum mechanical (QM) calculations on hydrogen terminated silicon nanowires (H−SiNWs) with optimized surfaces [usually {100} and {110}]. For each diameter, we determined both the best shape of the SiNW cross section and the optimum coverage of hydrogen. Then, we computed the band structure and relevant surface states and their scaling with diameter and surface hydrogen saturation.

RESULTS AND DISCUSSION

We show that there is a crossover from fully saturated hydrogen surfaces for $d < 1.9$ nm with valence and conduction band states delocalized over the NW to unsaturated hydrogen surfaces with valence and conduction wave functions localized on the surface. This leads to an evolution of the band gap with diameters consistent with experiment. These results are

Received: June 30, 2010
Revised: May 13, 2011
Published: May 17, 2011

 © 2011 American Chemical Society

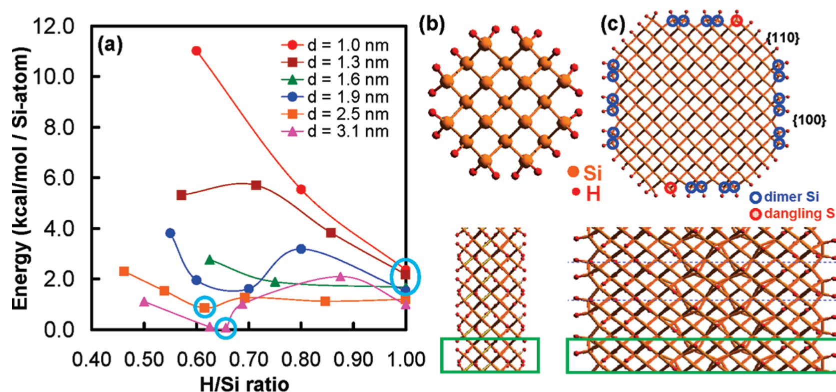

Figure 1. Optimized structures of H−SiNWs as a function of diameter. (a) Heats of formation vs H/Si ratio for 1.0 nm (red); 1.3 nm (brown); 1.6 nm (green); 1.9 nm (blue); 2.5 nm (orange); 3.1 nm (pink). We devine the H/Si ratio for each diameter so that the fully saturated case has H/Si =1. The minimum energy of each case is shown with light blue circles. (b) Cross section (top) and side view (bottom) for d = 1.0 nm, (H/Si = 1.00, $Si_{20}H_{21}$). The periodic unit length of 0.54 nm is shown with a green line. The square cross section is bounded by H saturated {110} surfaces on all four sides. (c) Cross section (top) and side view (bottom) for d = 3.1 nm (H/Si = 0.66, $Si_{196}H_{42}$) (orange, Si; red, H). Here we find an octagonal cross section with four {100} like surfaces leading to ten dimer Si atoms (shown with blue circles) as in the (2 × 2) reconstruction and two dangling Si atoms (shown with red circles). The four {110} surfaces are saturated as in (b).

relevant for characterizing and designing SiNWs for a range of applications.

We find that in a gas of hydrogen, H_2, the equilibrium surface structure for a [100] SiNW has both (001) and (011) surfaces facets, resulting in an octagonal shape. Most of the surface atoms prefer to bind to Si leading to one or two H's on each Si. However, in some cases, binding sufficient H to saturate each surface atom leads to too much strain, resulting in some surface Si atoms with 3 bonds plus a dangling singly occupied orbital. Correctly describing these states requires unrestricted or spin polarized wave functions that allow localized dangling bond orbitals to be singly occupied. In such cases, closed shell wave functions (every band orbital doubly occupied) can lead to large errors. For example, calculations of an unsaturated H−SiNW with diameter 2.5 nm ($Si_{129}H_{12}$), described in detail below, finds the closed shell Becke-3−Lee−Yang−Parr[20] (RB3LYP) energy is 1.58 eV higher than the wave function allowing singly occupied orbitals (unrestricted) UB3LYP. In this case, the closed shell wave function leads to a band gap of 0.39 eV compared to the UB3LYP value of 1.60 eV (Figures S4 and S5 of the Supporting Information, SI). Therefore, all of our calculations allowed spin polarization (UB3LYP).

The most fundamental property for designing SiNWs for electronics applications is the band gap, but it is well-known that DFT calculations often lead to band gaps too small by 1 or 2 eV. For example, the undoped cuprate La_2CuO_4 (an insulating spin-1/2 antiferromagnet) leads to zero band gap (a metal).[21−23] However, the B3LYP[20] flavor of density functional theory (DFT) leads to a band gap of 2.0 eV, in excellent agreement with experiment.[23] The reason is that the B3LYP hybrid functional includes 20% exact Hartree−Fock (HF) exchange in addition to the GGA exchange functionals.

All previously reported QM calculations of the band gaps of SiNWs used the LDA[24−26] or Perdew−Burke−Ernzerhof (PBE)[27−31] flavors of density functional theory with plane wave basis sets[24,25,27−32] which are known to lead to artificially low band gaps. Thus, we decided to calculate the band gaps of SiNWs using B3LYP, which has been shown to yield accurate band gaps for many systems.[23,33] A previous attempt to correct for the errors in LDA for Si NW used the GW method, but had to assume that there must be some universal dependence of band gap to the power of inverse of the diameter with no justification for this assumed relationship.[34] Another attempt modified the GGA Hamiltonian to include exact exchange, adjusting the fraction to agree with the band gap of bulk Si, but did not test whether it would provide accurate energetics.[35]

For plane wave basis sets commonly used for periodic boundary conditions (PBC) calculation of matrix elements with exact exchange is difficult. Thus codes such as VASP,[36] SIESTA,[37] ABINIT,[38] and ESPRESSO[39] cannot describe B3LYP wave functions. However, for PBC codes based on Gaussian basis sets (such as CRYSTAL[40] and SeqQUEST[43]), it is practical to include exact exchange. Thus, we used CRYSTAL[40] for the B3LYP band calculations on SiNWs. All calculations were performed with the 66−21G* basis sets for Si[41] and 3−1p1G for H,[42] which are of double-ζ plus polarization quality.[44]

We carried out structural geometry optimizations using the PBE functional with the SeqQUEST[43] PBC code (which uses Gaussian-basis functions), because PBE converges faster than B3LYP and SeqQUEST (which can treat PBE but not B3LYP) is much faster than CRYSTAL. These calculations used the PBE flavor of GGA[45] with PBE pseudo atomic potentials and spin polarization with no symmetry constraints. Six irreducible k-points in the Brillouin Zone were used. A real space grid spacing of 0.5 Bohr was used based on by energetic convergence and prior calculations of Si surfaces.[46]

We optimized the structures of H−SiNWs with diameters of 1.0, 1.3, 1.6, 1.9, 2.5, and 3.1 nm, using one-dimensional (1D) periodic boundary conditions with a unit cell of 5.4 Å in the wire direction [001]. We determined the optimum distribution of Si atoms and H termination by considering various distributions of surface Si and H atoms. Generally, we find that the NWs have an octagonal shape with four {100} plateaus that dimerize with no H and four {110} plateaus that have one H per Si (Figure S2 of the SI). At the edges between these 8 plateaus, there may be Si atoms bonded to one or two H atoms.

We calculated the heats of formation with respect to the energies of bulk Si and hydrogen molecules for each optimized H−SiNW structure. The results are shown in Figure 1a as a function of the rescaled H/Si ratio, where H and Si are the total

number of the atoms in the unit cell. For each diameter, we define the H/Si ratio so that H/Si =1 for the fully saturated case. For each diameter *d*, the most stable SiNW is shown with red circles. For $d \leq 1.9$ nm, we find that the hydrogen saturated surface, H/Si = 1, is most stable. This indicates that the hydrogen saturated surface is engetically more favorable than losing some of the hydrogen to the gas phase (hydrogen molecules). Thus it is favorable for hydrogen to react with the surface of SiNWs.

For $d = 1.0$ nm in Figure 1b, the most stable structure is $Si_{21}H_{20}$ with H/Si = 1.00. This has twelve surface Si atoms per unit cell where the middle Si atom has one H atom and the corner Si atoms have two H atoms. This leads to a heat of formation energy of $E_h = 2.4$ kcal/mol per Si. Hereafter, the units for the energy are per Si atom unless stated otherwise. Removing four H atoms per cell from the saturated SiNW leads to H/Si = 0.80, $Si_{21}H_{16}$, with two H terminated Si−Si dimers at two corners and $E_h = 5.5$ kcal/mol. Removing four more H atoms leads to an optimized H−Si [100] NW (H/Si = 0.60, $Si_{21}H_{12}$) with four dangling bond Si atoms in addition to the two Si−Si dimers with $E_h = 11.0$ kcal/mol. The detailed geometrical parameters of the H−SiNWs ($d = 1.0$ nm) are also shown in Figure S1 of the SI.

For $d = 2.5$ nm, the unsaturated H−SiNWs (H/Si = 0.62, $Si_{129}H_{32}$) is more stable than the saturated structure. It has eight H terminated Si dimers from the (2 × 2) reconstruction of the {100} surface and four dangling Si bonds at the corner per unit cell (Figure S3a of the SI).

For $d = 3.1$ nm, we find that the optimum NW has H/Si = 0.66 or $Si_{196}H_{42}$ with $E_h = 0.07$ kcal/mol. This H−SiNW is almost as stable as bulk Si plus hydrogen gas. It has 10 Si dimers paired along the {100} side walls with two dangling bonds at the corners and saturated termination on the {110} surfaces. This leads to two dangling bond Si atoms per unit cell (Figure 1c). Binding an H to these two dangling bond states increases the energy by 0.95 kcal/mol and is due to the Si strains and H−H interactions.

The structural parameters for all the H−SiNWs are in Table S1 of the SI. Saturated or equilibrium unsaturated models are shown in Figures S2 and S3 of the SI. H−SiNWs for $d = 2.5$ nm with various H/Si ratio are also shown in Figure S4 of the SI.

Table 1 and Figure S5 of the SI compare the experimental band gap of bulk Si crystal to the results of different functionals (B3LYP, PBE, and LDA). B3LYP leads to a direct Γ point band gap of 3.8 eV compared to 3.5 eV from experiment[47] while PBE leads to 2.6 eV and LDA leads to 2.4 eV. Similarly, the indirect band gap from B3LYP is 1.7 eV compared to 1.17 eV from experiment.[48] PBE is 0.4 eV and LDA is 0.2 eV. The reason for the improved band gaps for B3LYP is the inclusion of exact Hartree−Fock (HF) exchange that better accounts for the self-exchange hole.[22,23]

The band structures of the saturated H−SiNWs ($d = 1.0$ to 3.1 nm) all lead to a closed shell electronic structure as shown in Figure 2. The band gap ranges from 4.1 eV ($d = 1.0$ nm) to 2.2 eV ($d = 3.1$ nm). The valence band maximum (VBM) is always located at Γ just as in bulk Si. There are two classes of conduction band minimum (CBM), one at the Γ point that leads to a direct band gap for $d \leq 1.6$ nm and one ≈1/3 along Γ to X (the [100] direction) that leads to an indirect gap for $d > 1.6$ nm. However, even at $d = 3.1$ nm, the difference between the direct and indirect

Table 1. Band Gap of Si Crystal (eV) using Different Functional (B3LYP, PBE and LDA) Compared to Experimental Data

	B3LYP	PBE	LDA	experimental[a]
direct band gap	3.8	2.6	2.4	3.5
indirect band gap	1.7	0.4	0.2	1.17

[a] Refs 48 and 49

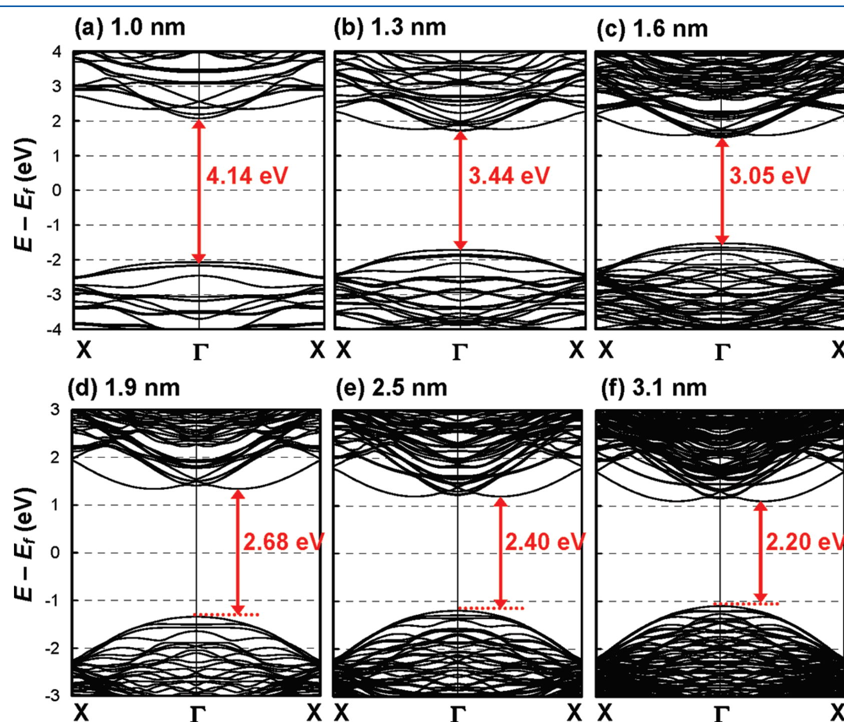

Figure 2. Band structures of saturated H−SiNWs using B3LYP. Diameter = (a) 1.0 nm, (b) 1.3 nm, (c) 1.6 nm, (d) 1.9 nm, (e) 2.5 nm, and (f) 3.1 nm. The VBM is at Γ just as in bulk Si. We find two classes of CBM, one at the Γ that leads to the direct band gap and one at 1/3 along the Γ to X. The latter leads to the indirect band gap. We find the smallest gap to be for $d \leq 1.6$ nm.

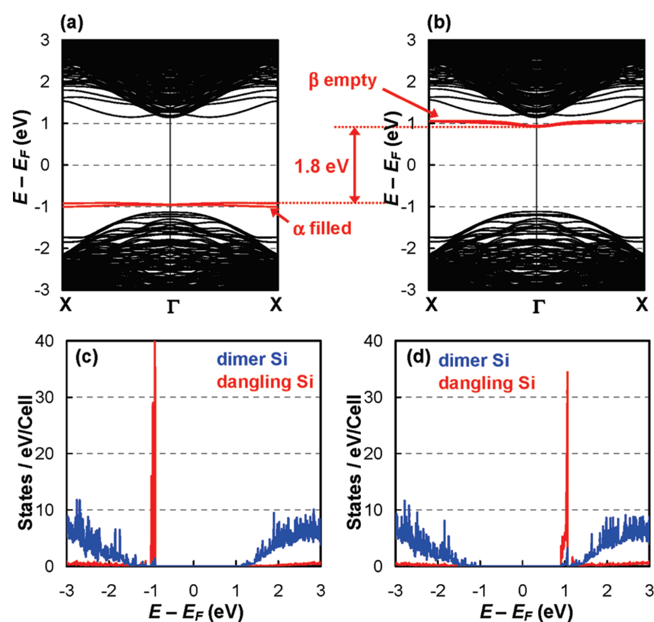

Figure 3. Band structures of the unsaturated H−SiNW with $d = 3.1$ nm ($Si_{196}H_{42}$) using UB3LYP. (a) α electrons and (b) β electrons. Partial density of states of Si atoms (per unit cell) of (c) α and (d) β electrons (blue; dimer Si atoms, red; dangling Si atoms). We find that the dangling bond Si atoms lead to new LUMO and HOMO states in the band gap.

Table 2. Effective Density of States Averaged Electron and Hole Masses (m^*_e and m^*_h) in Units of the Free Electron Mass of Saturated H-SiNWs as a Function of Diameter from B3LYP Calculations

	electrons m^*_e [a]		holes m^*_h
diameter (nm)	min along Γ to X [c]	Γ point	Γ point
1.0		**0.77**	18.28
1.3		**0.88**	16.94
1.6		**0.84**	5.59
1.9	**0.98**	0.71	2.64
2.5	**1.54**	0.69	2.51
3.1	**1.54**	0.59	2.29
Si bulk (B3LYP)	**1.63**	0.42	0.59 (heavy)
			0.34 (light)
Si bulk (exptl.) [b]	**1.08**		0.49 (heavy)
			0.16 (light)

[a] Values in boldface are the CBM. [b] ref 49. [c] For H−SiNWs at $d \geq 1.9$ nm, the CBM is at 33% from Γ to X.

band gap is only 0.06 eV, whereas in bulk Si the difference is 3.5 (CBM) − 1.2 (VBM) = 2.3 eV. A direct band gap for $d \leq 1.6$ nm opens the possibility of direct optical excitation without phonon emission, which is ideal for creating optical devices with SiNWs.

Table 2 shows the effective electron masses (m^*_e) and hole masses (m^*_h) of saturated H−SiNWs calculated from the band structures in Figure 2. We find that the effective masses approach the bulk values with increasing diameter. Here, the effective masses are derived by taking the geometric mean along the three directions. This is the value used in the density of states.

For $d = 3.1$ nm, the band structure and partial density of states (PDOS) of the most stable structure (H/Si = 0.21) calculated with UB3LYP (since they have two dangling-bond Si atoms per unit cell) are shown in Figure 3a,b. The PDOS of the α and β spin electrons show that the four dangling bond Si atoms lead to localized surface states for the HOMO and LUMO inside the band gap. The HOMO has spin α and the LUMO is spin β. The direct band gap is 1.8 eV. This is close to the calculated indirect band gap of bulk Si of 1.7 eV. These dangling bond Si sites are likely to attract group III or V dopants[30] to promote surface conductivity. We expect that this increased surface conductivity would further increase the thermoelectric figure of merit, ZT, in p-type SiNWs.[1,2]

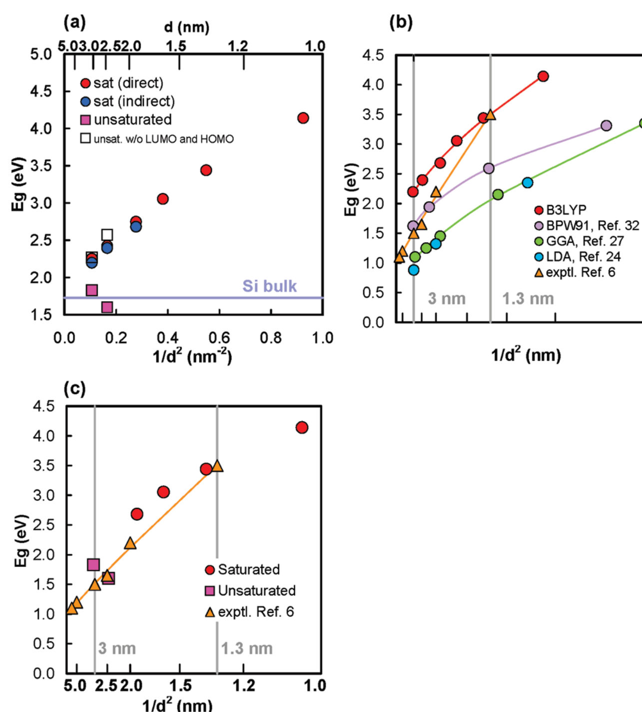

Figure 4. Band gap (E_g) as a function of $1/d^2$. (a) Calculated H−SiNWs band gaps using B3LYP. The red circles show the band gaps of saturated H−SiNWs. The blue circles show the indirect band gaps of saturated H−SiNWs. The orange squares show the band gaps of unsaturated H−SiNWs for $d = 2.5$ and 3.1 nm. The blank squares show the band gaps without the LUMO and HOMO created by the surface states of unsaturated H−SiNWs. (b) Comparison of our saturated B3LYP band gaps to other theoretical studies, LDA (blue circle, ref 24), GGA (green circle, ref 27), and BPW91 (purple circle, ref 32), on saturated SiNWs are shown. The experimental data (orange triangle; ref 6) is [011] for $d =$ 3 nm, otherwise [211]. The fit to experiment is not good because for diameters >1.9A, the equilibrium H−SiNW structure is unsaturated. (c) Plot of the lowest energy H−SiNWs structure band gaps (red circle, saturated at $d < 1.9$ nm; pink square, unsaturated at larger d) vs experimental data (orange triangle, ref 6). B3LYP and the correct SiNW structures explain the experimental data well.

The direct band gaps calculated by B3LYP as a function of squared diameter (d^2) in saturated H−SiNWs (red circle) are shown in Figure 4a. For $d \geq 1.6$ nm, the band gaps are indirect (blue circles) as described above. For $d = 2.5$ and 3.1, the equilibrium H−SiNWs structures have unsaturated hydrogen coverage. For $d = 3.1$, the band gap due to the surface dangling bonds is 1.9 eV, which is 0.2 eV smaller than the saturated H−SiNW of the same diameter. For $d = 2.6$, the band gap due to the surface dangling bonds is 1.6 eV, which is 0.8 eV smaller than the saturated H−SiNW of the same diameter. This 0.8 eV shift

occurs because of the quantum confinement is larger due to the reduced size of the reconstructed surface.[27]

Figure 4b shows the comparison of our results using B3LYP with previous theoretical studies on saturated H−SiNWs in the [001] growth direction[24,27,32] along with the known experimental values.[6] In addition, Figure 4c shows the known experimental band gaps[6] for H−SiNWs. These values are for the [112] growth direction except for d = 3.0 nm that was [110]. Prior calculations indicate that the band gaps of [001] NWs may be ∼0.2 eV smaller than those of [112] and [110].[24,27,32]

Clearly, the trend of the band gap on diameter from experiment disagrees dramatically with all QM calculations (see Figure 4b). If we neglected the hydrogen coverage dependence on diameter, our B3LYP calculations would also not agree with the trend from the experiment. As shown in Figure 4c, it is only when we combine the B3LYP band gap calculations with the optimum surface coverage that the theory matches with the experiment. For d = 1.3 nm, or smaller, we find that the SiNW surface Si are fully saturated with H, whereas for $d \geq 2.5$ nm, the SiNW has unsaturated surface Si atoms. Using the calculated optimum surface coverage, we find that B3LYP leads to excellent agreement with the experimental band gaps for the full range of the experiments.[6]

CONCLUSIONS

In summary, we have shown that the band gaps of SiNWs are dramatically affected by the diameter and the level of coverage by adsorbates (e.g., hydrogen) on the surface. We show that all previous QM calculations on H−SiNWs lead to both magnitude and trend of the energy gaps with diameter that disagree with experiment. In contrast, we find that using a thermodynamically stable level of hydrogen coverage in conjunction with B3LYP QM calculations leads to band gaps in good agreement with the experiment.

For diameters up to $d \approx 2$ nm, we find that the most stable level of hydrogen coverage is full saturation of surface Si bonds. For saturated H−SiNWs, we find that the QM band gaps from B3LYP scale inversely proportional to the diameter squared. We also show that there is a direct band gap for $d \leq 1.6$ nm and only a very small difference between the direct band and indirect band gaps for diameters up to 3.1 nm.

For $d \geq 2.5$ nm, we show that the equilibrium surface has a surface hydrogen coverage of ∼66% leading to dimer pair Si atoms (similar to the Si {100} surface) plus dangling bond trivalent Si atoms. These dangling bond atoms lead to donor and acceptor surface states that decrease the band gap by 0.2 to 0.8 eV with respect to the saturated surface. It is this crossover from fully saturated and unsaturated that is responsible for the steep dependence of the experimental band gap on diameter. Finally, the dangling bond states that are found to dominate the Si nanowires for diameters above 2.5 nm are relevant for understanding the possibility of topological insulator states in Si nanowire systems.

These results suggest that controlling the surface hydrogen coverage and diameter of SiNWs can be advantageous for tuning and enhancing optical performance, electrical conductivity, thermopower, and thermal conductivity. Similarly, the surface hydrogen atoms might be replaced by Cl, CH_3, or CCH to further tune other properties.[50,51] In particular, the low direct band gap nature of these small diameter SiNWs may provide useful photovoltaic properties for solar energy as well as optical and optoelectronic applications.[51]

ASSOCIATED CONTENT

Supporting Information. The structural parameters for all of the H−SiNWs are presented in Table S1. Saturated or equilibrium unsaturated models are shown in Figures S2 and S3. H−SiNWs for d = 2.5 nm with various H/Si ratio are also shown in Figure S4. Band structures of Si crystal calculated using (a) B3LYP, (b) PBE, and (c) LDA are in Figure S5. Band structures of the equilibrium H−SiNW with d = 2.5 nm (unsaturated) using UB3LYP (Figure S6) and RB3LYP (Figure S7). This material is available free of charge via the Internet at http://pubs.acs.org.

AUTHOR INFORMATION

Corresponding Author

*Phone: (626) 395-2731; (626) 395-2730 (Secretary). Fax: (626) 585-0918. E-mail: wag@wag.caltech.edu.

ACKNOWLEDGMENT

We thank Professor Seung Soon Jang and Professor Youyong Li for helpful discussions. This research was supported partially by DARPA-ONR PROM (00014-06-0938), NSF (CCF-0524490), and by the Microelectronics Advanced Research Corporation (MARCO) and its Focus Center Research Program (FCRP) on Functional Engineered NanoArchitectonics (FENA). W.A.G. is also supported by the WCU (NRF R-31-2008-000-10055-0) program funded by the Korea Ministry of Education, Science and Technology. The computer systems used in this research were provided by ARO−DURIP and ONR-DURIP.

REFERENCES

(1) Boukai, A. I.; Bunimovich, Y.; Tahir-Kheli, J.; Yu, J.- K.; Goddard, W. A., III; Heath, J. R. *Nature* **2008**, *451*, 168.

(2) Hochbaum, A. I.; Chen, R.; Delgado, R. D.; Liang, W.; Garnett, E. C.; Najarian, M.; Majumdar, A.; Yan, P. *Nature* **2008**, *451*, 163.

(3) Melosh, N. A.; Boukai, A.; Diana, F.; Gerardot, B.; Badolato, A.; Petroff, P. M.; Heath, J. R. *Science* **2003**, *300*, 112.

(4) Beckman, R.; Johnston-Halperin, E.; Luo, Y.; Green, J. E.; Heath, J. R. *Science* **2005**, *310*, 465.

(5) Mcalpine, M. C.; Ahmad, H.; Wang, D.; Heath, J. R. *Nat. Mater.* **2007**, *6*, 379.

(6) Ma, D. D. D.; Lee, C. S.; Au, F. C. K.; Tong, S. Y.; Lee, S. T. *Science* **2003**, *299*, 1874.

(7) Lu, W.; Lieber, C. M. *Nat. Mater.* **2007**, *6*, 841.

(8) Patolsky, F.; Timko, B. P.; Zheng, G.; Lieber, C. M. *MRS Bull.* **2007**, *32*, 142.

(9) Patolsky, F.; Zheng, G.; Lieber, C. M. *Nat. Protoc.* **2006**, *1*, 1711.

(10) Yang, C.; Barrelet, C. J.; Capasso, F.; Lieber, C. M. *Nano Lett.* **2006**, *6*, 2929.

(11) Tsakalakos, L.; Balch, J.; Fronoheiser, J.; Korevaar, B. A.; Sulima, O.; Rand, J. *Appl. Phys. Lett.* **2007**, *91*, 233117.

(12) Lieber, C. M.; Wang, Z. L.; et al. *MRS Bull.* **2007**, *32*, 99.

(13) Whang, D.; Jin, S.; Wu, Y.; Lieber, C. M. *Nano Lett.* **2003**, *3*, 1255.

(14) Javey, A.; Nam, S.; Friedman, R. S.; Yan, H.; Lieber, C. M. *Nano Lett.* **2007**, *7*, 773.

(15) Wu, Y.; Cui, Y.; Huynh, Y.; Barrelet, C. J.; Bell, D. C.; Lieber, C. M. *Nano Lett.* **2004**, *4*, 433.

(16) Li, C.-P.; Lee, C.-S.; Ma, X.-L.; Wang, N.; Zhang, R.-Q.; Lee., S. T. *Adv. Mater.* **2003**, *15*, 607.

(17) Holmes, J. D.; Johnson, K. P.; Doty, R. C.; Korgel, B. A. *Science* **2000**, *287*, 1471.
(18) Wang, C. X.; Hirano, M.; Hosono, H. *Nano Lett.* **2006**, *6*, 1552.
(19) Hirashita, N.; Kinoshita, M.; Aikawa, I.; Ajioka, T. *Appl. Phys. Lett.* **1990**, *56*, 451.
(20) Becke, A. D. *J. Chem. Phys.* **1993**, *98*, 5648. Stephens, P. J.; Devlin, F. J.; Chabalowski, C. F.; Frisch, M. J. *J. Phys. Chem.* **1994**, *98*, 11623.
(21) Tahir-Kheli, J.; Goddard, W. A., III *Phys. Rev. B* **2007**, *46*, 014514.
(22) Muscat, J.; Wander, A.; Harrison, N. M. *Chem. Phys. Lett.* **2003**, *342*, 397.
(23) Perry, J. K.; Tahir-Kheli, J.; Goddard, W. A., III *Phys. Rev. B* **2001**, *63*, 144510.
(24) Vo, T.; Williamson, A. J.; Galli, G. *Phys. Rev. B* **2006**, *74*, 045116.
(25) Peelaers, H.; Partoens, B.; Peeters, F. M. *Nano Lett.* **2006**, *6*, 2781.
(26) Aradi, B.; Ramos, L. E.; Deak, P.; Kohler, Th.; Bechstedt, F.; Zhang, R. Q.; Frauenheim, Th. *Phys. Rev. B* **2007**, *76*, 035305.
(27) Leu, P. W.; Shan, B.; Cho, K. *Phys. Rev. B* **2006**, *73*, 195320.
(28) Durgun, E.; Akman, N.; Ataca, C.; Ciraci, S. *Phys. Rev. B* **2007**, *76*, 245323. Durgun, E.; Cakir, D.; Akman, N.; Ciraci, S. *Phys. Rev. Lett.* **2007**, *99*, 256806.
(29) Nolan, M.; O'Callaghan, S.; Fagas, G.; Greer, J. G. *Nano Lett.* **2007**, *7*, 34.
(30) Fernandez—Serra, M. -V.; Adessi, Ch.; Blase, X. *Nano Lett.* **2006**, *6*, 2674.
(31) Ponomareva, I.; Menon, M.; Richter, E.; Andriotis, A. N. *Phys. Rev. B.* **2006**, *74*, 125311.
(32) Ng, M. -F.; Zhou, L.; Yang, S. -W.; Sim, L. Y.; Tan, V. B. C.; Wu, P. *Phys. Rev. B* **2007**, *76*, 155435.
(33) Matsuda, Y.; Tahir-Kheli, J.; Goddard, W. A., III *J. Chem. Phys. Lett.* **2010**, *1*, 2946.
(34) Rurali, R.; Aradi, B.; Frauenheim, Th.; Gali, A. *Phys. Rev. B* **2007**, *76*, 113303.
(35) Bruno, M.; Palummo, M.; Marini, A.; Del Sole, R.; Ossicini, S. *Phys. Rev. Lett.* **2007**, *98*, 036807.
(36) Kresse, D.; Furthmüller, J. *Comput. Mater. Sci.* **1996**, *6*, 15. Kresse, D.; Furthmüller, J. *Phys. Rev. B* **1996**, *54*, 11169.
(37) M Soler, J. M.; Artacho, E.; Gale, J. D.; García, A.; Junquera, J.; Ordejón, P.; Sánchez-Portal, D. *J. Phys.: Condens. Matter* **2002**, *14*, 2745.
(38) Gonze, X.; Beuken, J.-M.; Caracas, R.; Detraux, F.; Fuchs, M.; Rignanese, G.-M.; Sindic, L.; Verstraete, M.; Zerah, G.; Jollet, F.; Torrent, M.; Roy, A.; Mikami, M.; Ghosez, P.; Raty, J.-Y.; Allan, D. C. *Comput. Mater. Sci.* **2002**, *25*, 478.
(39) Baroni, S.; de Gironcoli, S.; Dal Corso, A.; Giannozzi, P. et al. , *The PWSCF Code*; DEMOCRITOS National Simulation Center of INFM: Trieste, Italy, 2008. http://www.quantum-espresso.org/
(40) Dovesi, R.; aunders, V. R.; Roetti, C.; Orlando, R.; Zicovich-Wilson, C. M.; Pascale, F.; Civalleri, B.; Doll, K.; Harrison, N. M.; Bush, I. J.; D'Arco, Ph.; Llunell, M., *CRYSTAL 06 User's Manual*; University of Torino: Torino, 2006. http://www.crystal.unito.it
(41) Gordon, M. S.; Binkley, J. S.; Pople, J. A.; Pietro, W. J.; Hehre, W. J. *J. Am. Chem. Soc.* **1982**, *104*, 2797. Binkley, J. S.; Gordon, M. S.; DeFrees, D. J.; Pople, J. P. *J. Chem. Phys.* **1982**, *77*, 3654.
(42) Gatti, C.; Saunders, V. R.; Roetti, C. *J. Chem. Phys.* **1994**, *101*, 10686.
(43) Schultz, P. A. *SEQQUEST code*; Sandia National Labs: Albuquerque, NM, 2005. http://dft.sandia.gov/Quest/.
(44) Mattsson, A. E.; Schultz, P. A.; Desjarlais, M. P.; Mattsson, T. R.; Leung, K. *Modelling Simul. Mater. Sci. Eng.* **2005**, *13*, R1–R31.
(45) Perdew, J. P.; Burke, K.; Ernzerhof, M. *Phys. Rev. Lett.* **1996**, *77*, 3865.
(46) Solares., S. D.; Michalak, D. J.; Goddard, W. A., III; Lewis, N. S. *J. Phys. Chem. B* **2006**, *110*, 8171.
(47) *Solid State Physics*; Ashcroft, N. W., Mermin, N. D., Eds.; W. B. Saunders Company: FL, 1997.
(48) *Physics of Semiconductor Devices*, 2nd ed.; Sze, S. M. John Wiley & Sons: New York, NY, 1981.
(49) *Electronic States in Crystal of Finite Size, Quantum Confinement of Bloch Waves*, Springer Tracts in Modern Physics 212; Ren, S. Y., Ed.; Springer: Heidelberg, Germany, 2006.
(50) Haick, H.; Hurley, P. T.; Hochbaum, A. I.; Yang, P.; Lewis, N. S. *J. Am. Chem. Soc.* **2005**, *128*, 8990.
(51) Bansal, A.; Li, X.; Lauermann, I.; Lewis, N. S. *J. Am. Chem. Soc.* **1996**, *118*, 7225.